Macromolecular Materials and Engineering
www.mame-journal.de

A Comparison Study of Fiber Diameter's Effect on Characteristic Features of Donepezil/Curcumin-Loaded Polycaprolactone/Polylactic Acid Nanofibers

*Saliha Aydin, Ilke Kabaoglu, Ece Guler, Fadime Topal, Ayse Nur Hazar-Yavuz, Ceyda Ekentok, Esra Tatar, Fatmanur Gurbuz, Oguzhan Gunduz, and Muhammet Emin Cam**

Nanofibers (NFs) offer an alternative option for the treatment of Alzheimer's disease (AD) by addressing unmet clinical problems. In this study, anti-AD drugs, donepezil (DO) and curcumin (CUR), are loaded in polylactic acid/polycaprolactone NFs. The effect of fiber diameter on drug release behavior is mainly observed, and the successful loading of DO and CUR to NFs is demonstrated. The tensile strength of DO/CUR-loaded NFs (DNFs) with lower fiber diameter is found to be higher. The working temperature is increased by the decrease of glass transition temperature and increase of the melting temperature after loading drugs. Furthermore, the increase in the percentage of swelling and decrease in the degradation rate for NFs are observed due to the increase of fiber diameter. Encapsulation efficiency and burst release percentages for DNFs are augmented by the increase of fiber diameter. Nevertheless, DNFs exhibit a sustained drug release manner over 2 weeks. NFs do not demonstrate a toxic effect on L929 (mouse fibroblast) cells, and additionally, they promote cell proliferation. Considering all these results, it is proven that the fiber diameter affects all characteristic features of NFs, and DNFs lead to a new and promising drug delivery system for the treatment of AD.

1. Introduction

Dementia is a progressive cognitive disorder that affects activities of daily living. Alzheimer's disease (AD), a form of dementia, is recognized as a global priority by the World Health Organization (WHO).[1] AD has complex pathogenesis, depending on various factors such as heredity, oxidative stress, vascular insufficiency, mitochondrial dysfunction, cholinergic disorders, neurotransmitter abnormalities, immunity, and environmental factors, which have not clearly explained yet.[2,3] Neurons lose their functions because of various factors such as the accumulation of β-amyloid plaques and defective τ proteins leading to neurofibrillary tangles that inhibit transmission of signals in patients with AD.[4,5] Furthermore, AD is also one of the most important causes of dementia that affects cognitive functions such as memory, speaking, problem-solving, and thinking. Moreover, it is estimated that the number of patients with AD will reach 106.8 million worldwide and 16.5 million in Europe by 2050.[4,6]

Although a lot of improvements in the treatment of AD have been made since the first case reported by Alois Alzheimer in 1907, a radical treatment has not yet been proven. Currently used medicines in the treatment of AD are memantine, donepezil (DO), rivastigmine, and galantamine.[4] Acetylcholinesterase in-

S. Aydin, I. Kabaoglu, E. Guler, F. Topal, A. N. Hazar-Yavuz, F. Gurbuz, M. E. Cam
Department of Pharmacology
Faculty of Pharmacy
Marmara University
Istanbul 34854, Turkey
E-mail: muhammet.cam@marmara.edu.tr

S. Aydin, I. Kabaoglu, E. Guler, F. Topal, O. Gunduz, M. E. Cam
Center for Nanotechnology and Biomaterials Application and Research
Marmara University
Istanbul 34722, Turkey

C. Ekentok
Department of Pharmaceutical Biotechnology
Faculty of Pharmacy
Marmara University
Istanbul 34854, Turkey

E. Tatar
Department of Pharmaceutical Chemistry
Faculty of Pharmacy
Marmara University
Istanbul 34854, Turkey

O. Gunduz
Department of Metallurgy and Material Engineering
Faculty of Technology
Marmara University
Istanbul 34722, Turkey

The ORCID identification number(s) for the author(s) of this article can be found under https://doi.org/10.1002/mame.202100855

DOI: 10.1002/mame.202100855

hibitors (AChEIs) that increase the acetylcholine level by preventing the breakdown of acetylcholine in synapses are the basis of symptomatic treatment.[1] One of the selective AChEIs, which are frequently used in all stages of AD as well as vascular and Parkinson's-related dementia, is DO hydrochloride.[7]

Investigations on alternative treatments are significantly important because of insufficient approved drugs for AD treatment. It has been reported that oxidative stress prevents healthy aging and causes various diseases such as AD.[8] Curcumin (CUR) reduces oxidative stress and inflammation, and has positive effects on neuronal and vascular functions. It shows its main effect by binding to β-amyloid plaques in the central nervous system; consequently, the accumulation of these plaques and their transformation to neurotoxic species is reduced.[9]

Drugs that are either orally administered in the form of tablets, capsules, and granules, or used parenterally such as intravenous, subcutaneous, and intramuscular have some disadvantages such as the first-pass effect or pain at the injection site, respectively. Nowadays, it has been observed that polymeric nanofibers (NFs) play a key role in drug delivery systems with a fewer disadvantages.[10] Since it is very crucial to design an appropriate drug delivery system with a controlled release capability, controlled drug release from NFs has gained importance in the development of new methods to increase biosolubility and bioavailability by decreasing the amount of drug administered.[11,12]

Electrospinning (ES), an electro-hydrodynamic atomization method that can be used for scale production of nanofibers in industrial applications, is used to create ultrafine fibers using an electrostatic potential characterized by high voltage and very low current.[13,14] ES is widely used to produce polymeric NFs in different diameters by changing solution properties and process control parameters.[15] Natural polymers like gelatin, chitosan, and alginate, and synthetic polymers such as poly(ε-caprolactone) (PCL) and polylactic acid (PLA) are used to produce NF by ES. NFs are produced after the evaporation of solvent which is used by exposing high electrical voltage in this technique.[11]

PLA is a biodegradable, biocompatible, bioabsorbable, hydrophobic, synthetic, and semicrystalline aliphatic polymer. PLA, which has three isomeric forms ((D), (L), and racemic (D,L)), is a semicrystalline solid that has been approved by the Food and Drug Administration (FDA) for biomedical usage.[16] PLA attracts much attention due to showing controlled-manner drug release and maintaining high stability over a long period.[17] Furthermore, it shows lower degradation properties due to its high hydrophobicity and crystallinity properties compared to PLA.[16] The physical, mechanical, and thermal properties and the degradation rate of PCL are affected by its molar mass and crystallinity degree. Also, it can be combined with other polymers such as PLA to improve its biodegradability, tensile strength, drug release, swelling, and thermal behaviors.[17]

The treatment of AD is challenging because of the complex pathophysiology of the disease, and also drug-related and patient compliance problems. The studies concerning new drug delivery systems such as NFs for the effective and advantageous treatment of AD are at the basis of current research topics that arouse interest in the literature. Gencturk et al. manufactured polyurethane hydroxylpropyl cellulose NFs that can be used as a carrier system for the transfer of DO across the skin.[18] In another study by AnjiReddy and Karpagam, anti-Alzheimer's effect of DO-loaded chitosan NFs was evaluated.[19] Perumal et al. produced CUR-loaded PLA/hyperbranched polyglycerol NFs for wound-dressing applications.[20] As part of these studies on NFs produced by ES, assays such as methylthiazolydiphenyl-tetrazolium bromide (MTT), differential scanning calorimeter (DSC), Fourier transform infrared spectroscopy (FTIR), X-ray diffraction (XRD), and tensile tests have been evaluated, and successful results have been obtained. In the light of the foregoing literature, we aimed to obtain a promising carrier system for an effective combination therapy with DO and CUR loaded in PLA/PCL NFs for the treatment of AD.

In our study, CUR, was obtained from *Curcuma longa*, and DO was loaded in PLA/PCL NFs at different polymer concentrations. Mainly, the drug release kinetics of NFs were evaluated to analyze the effect of NF diameter on drug release behavior. Moreover, the properties of the polymer solutions of NFs were evaluated by measuring the physical parameters like electrical conductivity, surface tension, viscosity, and density. Crystalline, chemical, and morphological properties of all electrospun NFs were examined with XRD, scanning electron microscopy (SEM), and FTIR, respectively. The mechanical and thermal properties of NFs were also analyzed. The MTT viability test was used to detect the effect of NFs on cell proliferation. Also, encapsulation efficiency (EE), degradation rate, and swelling ratio of NFs were investigated.

2. Experimental Section

2.1. Materials

DO ($M_w \approx 379.5$ g mol^{-1}), PCL (M_w: 80.000 g mol^{-1}), methanol (99.8% purity, v/v), and Tween 80 were bought from Sigma Aldrich (UK). PLA (M_w: 110.000 g mol^{-1}) was purchased from NatureWorks LLC, Minnetonka, MN. Phosphate-buffered saline (PBS) tablets (pH = 7.4) were purchased from Chembio (Istanbul, Turkey). Chloroform was bought from Merck KgaA (Darmstadt, Germany). All reagents were of analytical quality.

2.2. Plant Material and Preparation of Plant Extracts

Curcuma longa rhizomes were purchased from the Istanbul province of Turkey. An oven set at 105 °C was used to dry the rhizome parts of *C. longa*. Subsequently, it was sieved to obtain a more homogeneous extract. The plant powder was preserved in the refrigerator to prevent humidity. Later, it was extracted by using the Soxhlet apparatus. Extraction was performed as follows: plant powder was poured into a thimble, then placed in the Soxhlet apparatus which was slowly filled by acetone, which was used as extraction solvent. This experiment was performed for 8 h at a constant temperature at 60 °C. After completion of the extraction process, acetone was separated from the extract using a rotary evaporator under a vacuum at 35 °C.[21]

2.3. Preparation and Characterization of Solutions

PLA and PCL were dissolved in chloroform:methanol mixture (3:1 v/v) at different concentrations (8%, 12%, and 15% (w/v)).

Table 1. Flow rate, voltage, and working distance for pure and DO/CUR-added PLA/PLC NFs at different concentrations.

Samples	Flow rate [mL h^{-1}]	Voltage [kV]	Working distance [mm]
Pure 8% PLA/PCL NF (PNF8)	3	26.8	150
Pure 12% PLA/PCL NF (PNF12)	4	26.8	150
Pure 15% PLA/PCL NF (PNF15)	5	26.8	150
DO/CUR-loaded 8% PLA/PCL NF (DNF8)	3	27.1	150
DO/CUR-loaded 12% PLA/PCL NF (DNF12)	4	28.9	120
DO/CUR-loaded 15% PLA/PCL NF (DNF15)	5	31.2	120

Following, PLA and PCL were mixed at a ratio of 4:1 (v/v) as the uniform morphology of all pure NFs' (PNFs) formation was obtained at this ratio in the SEM images. Later, DO (5 mg mL^{-1}) and CUR (2 mg mL^{-1}) were mixed and added to PLA/PCL (4:1 v/v) pure solutions at the concentrations of 8%, 12%, and 15% (w/v), separately. In addition, 1% (w/v) Tween 80 was added to the solutions and mixed slowly. Thus, each of DO/CUR-loaded NFs (DNFs) and PNFs was produced at three different concentrations.

Some physical parameters of all solutions were evaluated. A density bottle (10 mL specific density bottle, Boru Cam Inc., Turkey), an electrical conductivity probe (Cond 3110 SET 1, WTW, Germany), a viscometer (DV-E, Brookfield AMETEK, USA), and a force tensiometer (Kruss K9, Hamburg, Germany) were used. The calibration processes of the devices were carried out at ambient temperature (25 °C) before the experiment. Measurements were made in the same environment and repeated three times.

2.4. Production of Nanofibers

PNFs and DNFs were produced by ES in different process parameters such as voltage, working distance from needle tip to a metal plate, and flow rate (**Table 1**). Flow rate, voltage, and working distance were applied between 3 and 5 mL h^{-1}, 26.8–31.2 kV, 120–150 mm, respectively.

2.5. Scanning Electron Microscopy

The size and morphology of NFs were determined by using SEM (EVO LS 10, ZEISS, USA). First, the surfaces of the samples were coated with gold for 1 min and then analyzed at 10 kV accelerating voltage and 23 mm working distance. Then, the average diameter and size distribution of NFs were measured with Image J (Brocken Symmetry Software) by analyzing 100 NFs in SEM images recorded randomly.[22]

2.6. Tensile Test

An Instron 4411 tensile tester (MA, USA) was used to test the tensile strength of NFs. This process was carried out at 23 °C. Data were analyzed with Bluehill 2 software (Elancourt, France). A digital micrometer was utilized to examine the thickness of NFs. For this test, six samples (10 × 50 mm) were taken from each NF group. The upper and lower handles were clamped on both ends of each sample. Samples were subjected to the tensile test until the breaking point and 10 mm grip width under conditions of 5 mm min^{-1} test speed.

2.7. Fourier Transform Infrared Spectroscopy

To suggest whether PNFs and DNFs had all essential components to form NFs, their FTIR spectra were recorded. The Jasco FTIR 4700 spectrometer was used for FTIR measurements, and the OPUS Viewer version 6.5 was used to interpret the spectra. The spectra were recorded from 500 to 4000 cm^{-1} at room temperature with a resolution of 4 cm^{-1}.

2.8. X-Ray Powder Diffraction

Crystal forms and structures of PLA, PCL, DO, and CUR were analyzed at 2° min^{-1}, 40 mV, and 30 mA. For this, Cu Kα radiation and a D/Max-BR diffractometer (RigaKu, Tokyo, Japan) were used. The same process was repeated for PNFs and DNFs at different concentrations. Conversion of the resulting data into diffractograms was done with the OriginPro 7.0 software (OriginLab Corporation, MA, USA).

2.9. Differential Scanning Calorimeter

DSC analysis, which is used for the characterization of the thermal properties of the material, was performed under the dynamic argon atmosphere (20 mL min^{-1}) at a heating rate of 10 °C min^{-1} between 0 and 200 °C using PerkinElmer Inc Jade DSC and Pyris software (MA, USA). Also, the glass transition temperature (T_g) and melting temperature (T_m) of PNFs and DNFs were analyzed using DSC. Since the melting enthalpy and the melting point of indium affect temperature calibration, the calibration in DSC was adjusted accordingly.

2.10. Determination of Drug Encapsulation Efficiency

DO and CUR contents in NFs were defined according to the standard assay procedure. Briefly, all DNFs, each weighing an average of 5 mg, were dissolved in 10 mL solvent mixtures. The flask was stirred at a constant rate for an hour to release the drugs from the NFs. A solution of 1 mL was taken, and a UV spectrophotometer (Shimadzu UV-3600, Japan) was used to detect DO and CUR in NFs at 271 and 426 nm.[23,24] The EE was calculated in line with Equation (1). All measurements of samples were repeated in sets of three

$$\text{Encapsulation efficiency} = \frac{\text{Mass of actual drug loaded in nanofibers}}{\text{Mass of drug used in nanofibers' fabrication}} \times 100 \quad (1)$$

Table 2. The drug release kinetic mathematical models and their equations (in these equations, Q is the fractional amount of drug release at a time t, where K_0, K_1, and K_{HC} are the kinetic constants for zero-order, first-order, and Hixson–Crowell models, respectively).

Kinetics model	Equations
Zero order	$Q = K_0 t$
First order	$\ln(1 - Q) = -K_1 t$
Hixson–Crowell	$Q_{1/3} = K_{HC} t$

2.11. In Vitro Drug Release Assay

In vitro drug release tests of DNFs at different concentrations (8%, 12%, and 15%, w/v) were examined, and their release kinetics were analyzed. Before starting the tests, linear calibration curves of DO and CUR solutions at 2, 4, 6, 8, and 10 µg mL^{-1} concentrations were evaluated.

All samples, of ≈5 mg, were placed in 1 mL of PBS at pH 7.4 and 37 °C, and kept in a rotary shaker at 250 rpm throughout the assay. 1 mL of PBS was collected from each of DNF samples and replaced with 1 mL of fresh PBS at 0, 1, 1.5, 2, 3, 4, 6, 8, 12, 24, 48, 72, 96, 120, 144, 168, 192, 216, 240, 264, 288, 312, and 336 h. DO and CUR releasing profiles from DNFs at different polymer concentrations (8%, 12%, and 15%, w/v) were detected at 271 and 426 nm by a UV spectrophotometer (Jenway 7315, Bibby Scientific, Staffordshire, UK), respectively.[23,24]

2.12. In Vitro Drug Release Kinetics

DNFs were analyzed using three different mathematical models, which were zero-order, first-order, and Hixson–Crowell to mimic their drug release kinetics.[25] The equations belong to the drug release kinetic mathematical models that are shown in **Table 2**.

2.13. Swelling and Degradation Behaviors

To evaluate swelling rates, all NFs were dipped in PBS at pH 7.4 and 37 °C. During the test, three samples of each NF group dipped in 1 mL of PBS were kept in a 37 °C thermal shaker (BIOSAN TS-100). On the first day, the initial weights of NFs (W_0) were calculated and then, the wet weights (W_w) of the samples were measured at 30th min, and at 1st, 2nd, 3rd, 8th, and 24th h for the swelling test. Equation (2) was used to calculate the swelling value (S)[26]

$$S = \frac{W_w - W_0}{W_0} \times 100 \quad (2)$$

NFs were dried for 6 h under ambient conditions after they were taken from PBS medium (pH 7.4) and weighted (W_t) at the determined time (1st, 4th, 10th, and 12th; 5th, 9th, 13th, 17th, and 21st day) for the degradation test. Equation (3) was used to calculate the degradation level (D_i)[26]

$$D_i = \frac{W_0 - W_t}{W_0} \times 100 \quad (3)$$

2.14. MTT Viability Assay

L929 cells were cultured in Dulbecco's modified Eagle's medium (supplemented with 10% fetal bovine serum). After that, they were seeded in 48-well plates at a density of 2.5×10^4 cells per well. They were then cultured at 37 °C, 5% CO_2 overnight. Cells were incubated with NF samples for 48 h. After 48 h of treatment with NFs, the culture medium was replaced with a fresh medium and then 20 µL of MTT solution was added to wells. The plate was incubated at 37 °C and 5% CO_2 for 4 h, and the formazan crystals were solubilized by adding 200 µL solubilization buffer, and spectrophotometric absorbance was measured at 271 and 428 nm.[23,24] The confluent cells were used in cytotoxicity tests and SEM investigations.

2.15. Statistical Analysis

GraphPad Prism 6 statistics program was used to perform statistical analysis of the data, which were collected from the results of each experiment. The consequences of the examination were given as mean ± standard deviation. One-way and two-way analysis of variance (ANOVA) and the Tukey posthoc test were used for the intergroup evaluations. p-values of <0.05 were statistically significant.

3. Results and Discussion

3.1. Characterization of Polymer Solutions

Working distance, flow rate, and electrical voltage are the parameters that affect NF production in the ES technique. Besides environmental parameters as ambient temperature and relative humidity, and solution physical parameters such as solvent type, polymer concentration, electrical conductivity, surface tension, density, and viscosity have crucial effects on characterization and morphology of NFs.[27] Fiber diameter changes are concurrent with the changes in characterization and morphology of NFs.[28,29] Addition of DO and CUR to PLA/PCL solutions changed the physical parameters of these solutions. The changes in electrical conductivity, surface tension, viscosity, and density of the solutions resulted from adding drugs were given in Figure S1 (Supporting Information). The densities of PNF8, PNF12, and PNF15 solutions were measured at 1.33, 1.34, and 1.35 g mL^{-1}, respectively. The densities of DNF8, DNF12, and DNF15 solutions were measured as 1.34, 1.37, and 1.38 g mL^{-1}, respectively. It was proven that the density of the solutions increased concurrently with the polymer concentration. Also, following the addition of DO/CUR, an increase in the solution density was observed. Surface tensions of PNF8, PNF12, PNF15, DNF8, DNF12, and DNF15 solutions were 25.6, 27.8, 25.2, 34.4, 72.9, and 126.0 mN m^{-1}, respectively. The viscosities of PNF8, PNF12, and PNF15 were 6420, 7034, and 7810 mPa s, respectively, and the viscosities of DNF8, DNF12, and DNF15 solutions were 7564, 8545, and 8640 mPa s, respectively. The electrical conductivities of PNF8, PNF12, PNF15, DNF8, DNF12, and DNF15 solutions were measured as 0.9, 1.0, 0.8, 40.7, 37.2, and 36 µS cm^{-1}, respectively. The addition of drugs in polymer solutions resulted in increased viscosity, surface tension, electrical conductivity, and density values.

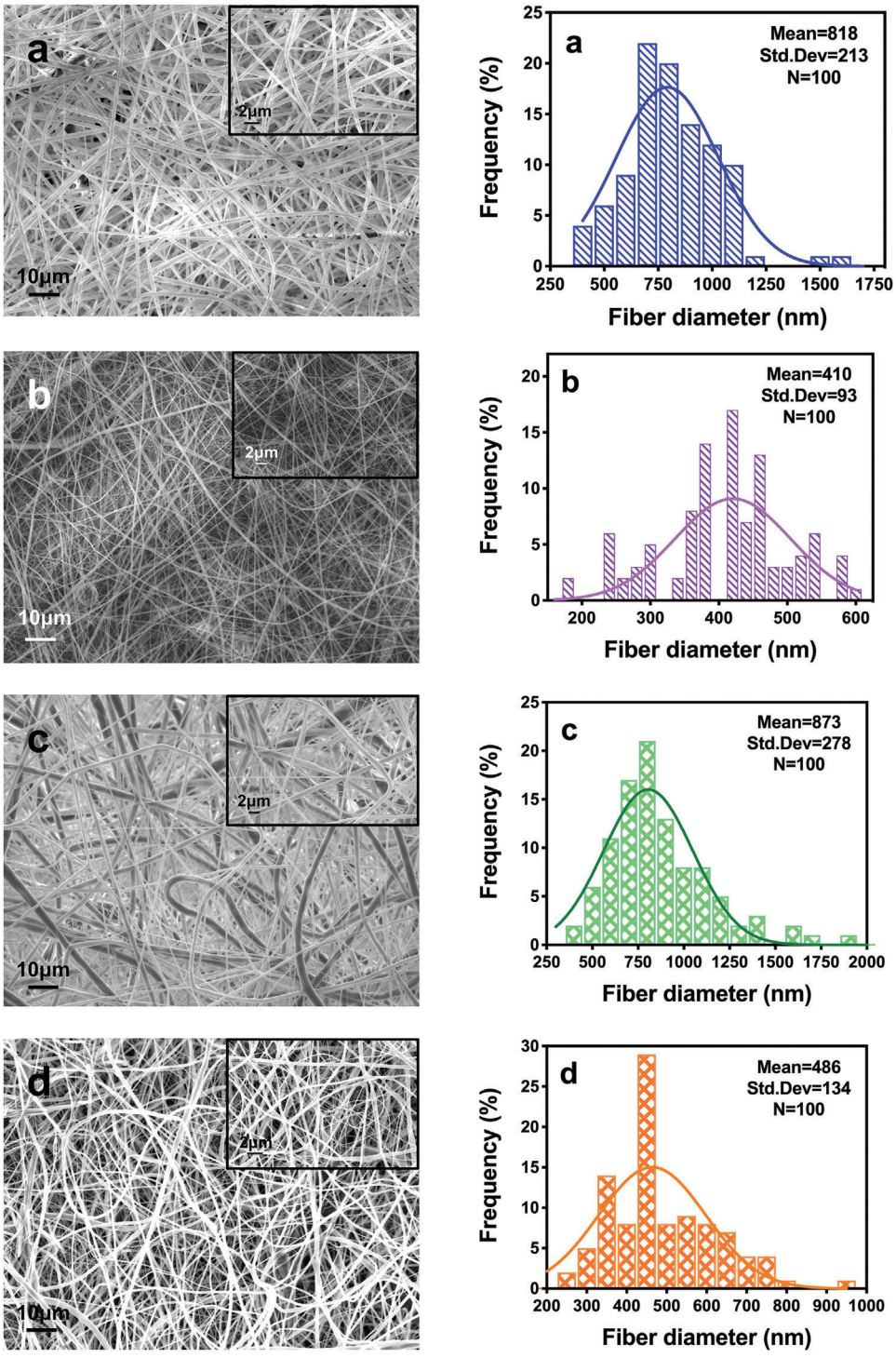

Figure 1. Scanning electron microscopy (SEM) images and diameter distributions of pure and donepezil (DO)/curcumin (CUR)-loaded nanofibers (NFs) at different concentrations (8%, 12%, and 15%). a1,a2) Pure 8% polylactic acid (PLA)/polycaprolactone (PCL) NF (PNF8). b1,b2) DO/CUR-loaded 8% PLA/PCL NF (DNF8). c1,c2) Pure 12% PLA/PCL NF (PNF12). d1,d2) DO/CUR-loaded 12% PLA/PCL NF (DNF12), e1,e2) Pure 15% PLA/PCL NF (PNF15), and f1,f2) DO/CUR-loaded 15% PLA/PCL NF (DNF15). In all diameter distributions, $n = 100$.

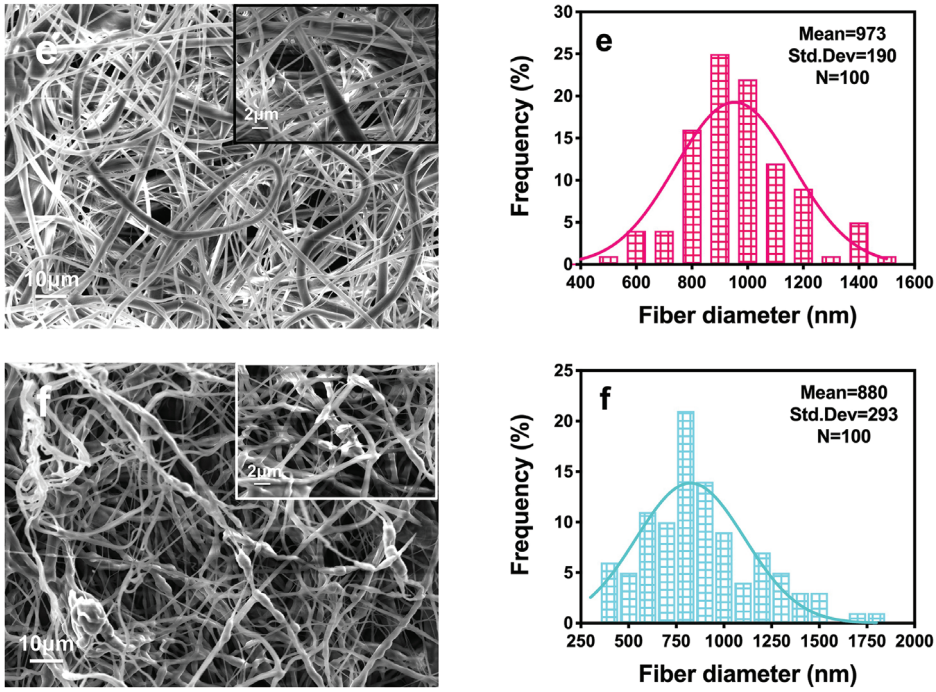

Figure 1. *Continued*

3.2. Process Conditions

To produce NFs by using ES, the voltage, flow rate, and distance were utilized between 26.8 and 31.3 kV, 3–5 mL h^{-1}, and 120–150 mm, respectively. The voltage and flow rate applied to solutions rose concurrently with the increasing concentration of solutions. Furthermore, after the addition of drugs to PNF8, PNF12, and PNF15, higher voltages (27.1, 28.9, and 31.2 kV) were applied compared to PNFs (26.6, 26.7, and 26.8 kV), respectively. The gap between the top of the collector and needle remained constant at 150 mm for all NFs except DNF12 and DNF15 in which 120 mm was applied.

3.3. Morphological Characterization of NFs

According to Son et al., the diameters of NFs raise concurrently by increasing the concentrations of solutions.[30] In this study, NFs were produced by using PLA/PCL polymer composite in different concentrations, and then, the diameters and morphological structure of these NFs were compared by using SEM (**Figure 1**). The diameters of PNF8, PNF12, and PNF15 were measured 818 ± 213, 873 ± 278, and 973 ± 190 nm, respectively. On the other hand, after loading DO/CUR in NFs, the diameters of NFs decreased to 410 ± 93, 486 ± 134, and 880 ± 293 nm, respectively. Thus, it was proven that the diameters of PNFs were thicker than DNFs. The aforementioned result was found in the literature.[31] Furthermore, increased surface tension and viscosity and decreased electrical conductivity of the solutions reveal larger fiber diameters.[32,33] Although solution viscosity and surface tension increased by the addition of drugs, the increase in electrical conductivity caused the fiber diameter to decrease for DNFs.

3.4. Fourier Transform Infrared Spectroscopy

FTIR, a spectroscopic method, is used to show characteristic vibrational absorption bands of chemical structures and interactions of compounds. FTIR spectra of pure DO, CUR, PLA, PCL, PNFs, and DNFs are given in Figure S2 (Supporting Information). FTIR spectra exhibited characteristic absorption bands of pure DO at 3585.0, 3361.3, 2921.6, 2858.0, 1681.6, and 1066.4 cm^{-1} that were ascribed to N–H bond, O–H bond, asymmetric and symmetric C–H bonds of the methyl group, C═O bond, and C–O bond stretching, respectively.[34] The characteristic bands of CUR, OH stretching vibration at 3232.1 cm^{-1}, $-CH_3$ stretching vibration at 2906.2 cm^{-1}, C–O stretching vibration at 1024.0 cm^{-1} were also detected.[35] The vibrations belonging to pure PLA were recorded at 2901.2, 2889.7, 1747.2, 1266.0, and 1128.2 cm^{-1}, respectively. On the other hand, the vibrations of pure PCL were observed at 2940.9, 2865.7, 1722.1, 1238.1, and 1165.8 cm^{-1}, respectively. The vibrations belonging to these two polymers are CH asymmetric stretching, CH symmetrical stretching, C═O stretching, CH bending, and C–O stretching, respectively. According to the FTIR analysis, the characteristic bands of all drugs and polymers were observed in the FTIR spectra of all produced PNFs and DNFs. Therefore, the gathered data revealed that the produced NFs have successfully been produced.[34]

3.5. X-Ray Powder Diffraction

XRD is used to examine the crystalline structure of the samples. The XRD results of pure PLA, PCL, DO, CUR, PNFs, and DNFs are demonstrated in **Figure 2**. The peaks seen in the CUR and DO graphs could be interpreted as both having a crystalline structure. The characteristic peaks of DO were observed at 12.6°, 21.1°, and

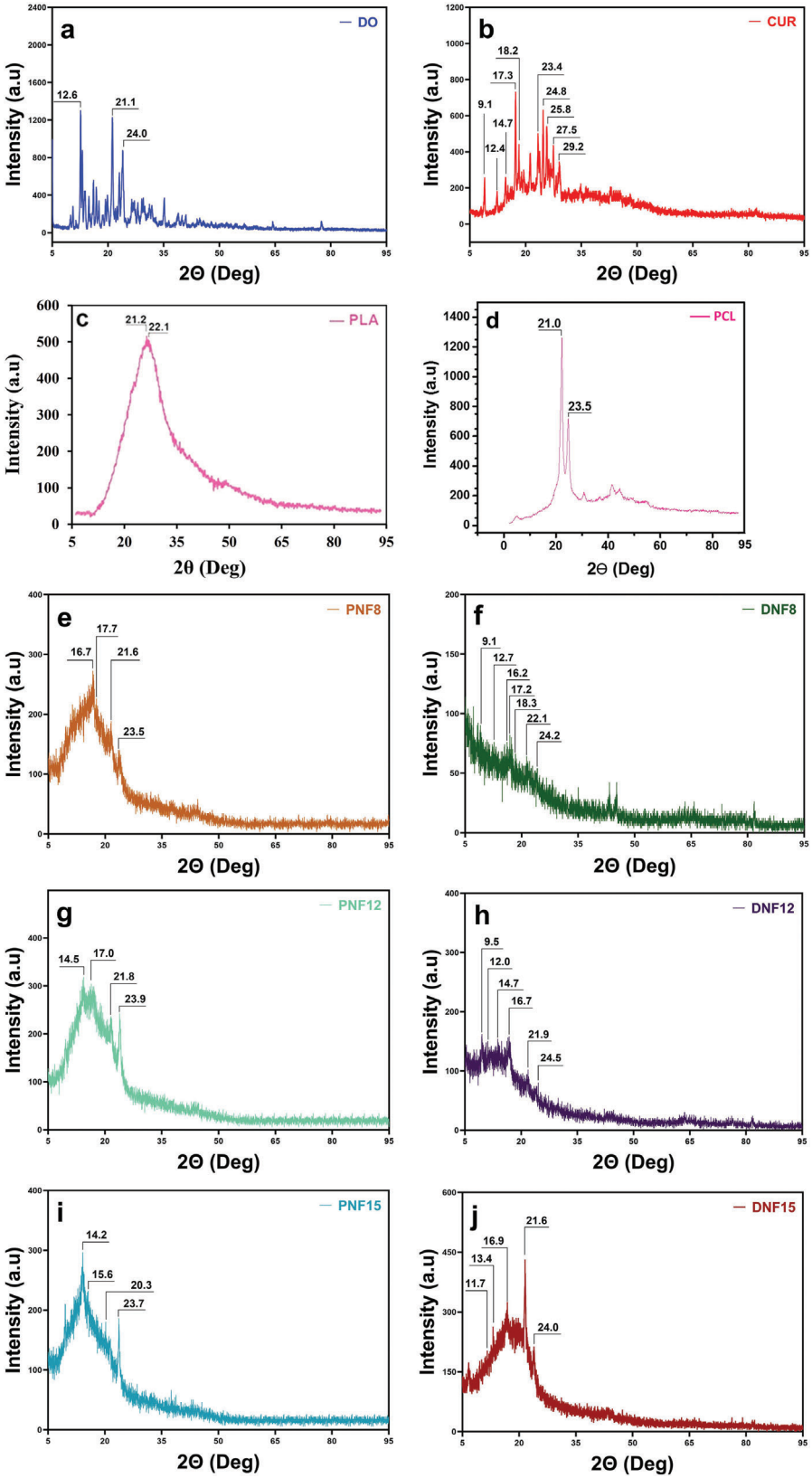

Figure 2. X-ray diffraction (XRD) patterns of a) pure donepezil (DO), b) pure curcumin (CUR), c) pure polylactic acid (PLA), d) pure polycaprolactone (PCL), e) pure 8% PLA/PCL nanofiber (NF) (PNF8), f) DO/CUR-loaded 8% PLA/PCL NF (DNF8), g) pure 12% PLA/PCL NF (PNF12), h) DO/CUR-loaded 12% PLA/PCL NF (DNF12), i) pure 15% PLA/PCL NF (PNF15), and j) DO/CUR-loaded 12% PLA/PCL NF (DNF15).

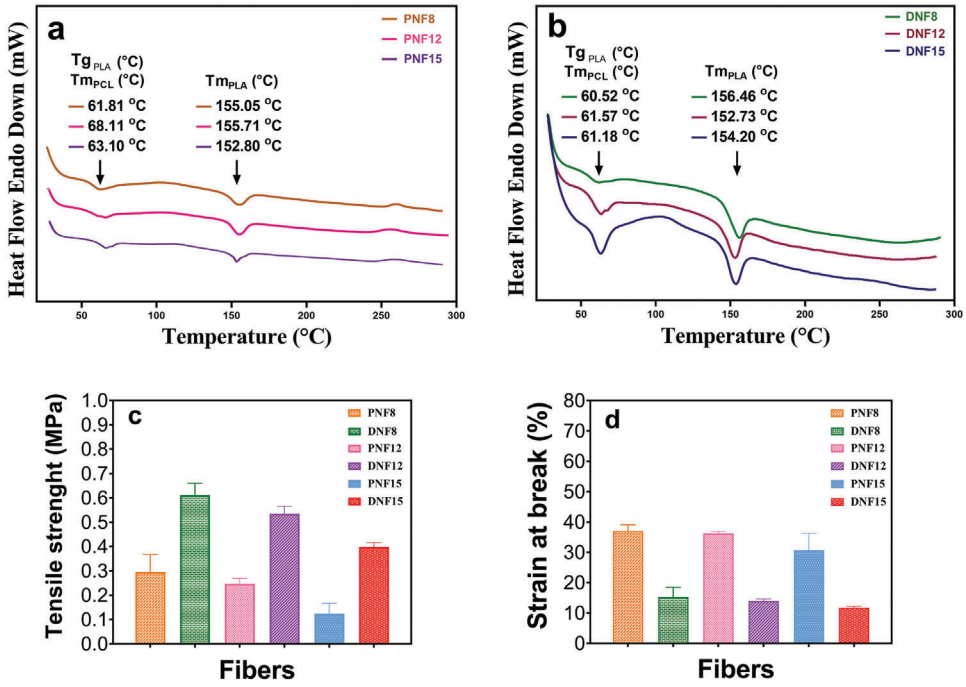

Figure 3. Differential scanning calorimetry (DSC) curves of a) pure 8%, 12%, and 15% polylactic acid/polycaprolactone (PLA/PCL) nanofibers (NFs) (PNF8, PNF12, and PNF15, respectively); and b) donepezil/curcumin-loaded 8%, 12%, and 15% PLA/PCL NFs (DNF8, DNF12, and DNF15, respectively). Tensile properties of NFs: c) tensile strength and d) strain at break.

24.0° 2θ,[36] and CUR was detected at 9.1°, 12.4°, 14.7°, 17.3°, 18.2°, 23.4°, 24.8°, 25.8°, 27.5°, and 29.2° 2θ. Thus, it was proven that the DO and CUR appear in the crystalline structure.[37,38]

The peaks for pure PLA were observed at 21.2° and 22.1° 2θ, while peaks for pure PCL were obtained at 21.0° and 23.5° 2θ, respectively. The presence of sharp peaks of PCL indicated that it has greater crystallinity than PLA.[22] However, PLA appeared to have an amorphous or slightly crystalline structure. The fact that PLA gave a few peaks that were not sharp has indicated that PLA is far from the crystalline structure.[39,40]

In this study, according to the XRD results obtained from the PNFs, the peaks belonging to PLA were seen between 13° and 17° 2θ, and the peaks belonging to PCL were seen between 20° and 24.5° 2θ. According to the studies of Sun et al., PLA crystallization is affected by the addition of small amounts of PCL.[41] It is clearly seen that the peaks belonging to PLA were observed at 16.7° and 17.7° 2θ in PNF8, and the peak positions shifted to lower positions at "14.5° and 17.0° 2θ" and "14.2° and 15.6° 2θ" in PNF12 and PNF15, respectively. As a result, in the current study, the peak positions of PLA shifted to a lower 2θ after mixing with higher PCL concentration.

The characteristic peaks belonging to DO and CUR were observed in DNFs, and it was proved that DO and CUR were successfully loaded with NFs.

3.6. Differential Scanning Calorimetry

DSC is one of the analyses used to obtain significant information about the thermal activity and phase transition of materials. With the help of this technique, the presence of ingredients and their physical conditions in formulations were examined. The changes in T_g and T_m of polymers are two remarkable factors caused by the conditions of manufacture and additives present in the formulation.[42] In this study, T_g and T_m values were measured between the range of 0 and 300 °C by DSC analysis. The DSC curves were constructed for the evaluation of thermal properties of PNF8, PNF12, PNF15, DNF8, DNF12, and DNF15 shown in **Figure 3**a,b. While the T_m values of PCL were observed around 60 °C, the T_g and T_m values of PLA were found between 50—80 and 150—180 °C.[43,44] In PNF8, PNF12, and PNF15 samples, there were endothermic peaks at 61.8, 68.1, and 63.1 °C. These peaks can be caused by the overlapping of PCL's T_m point and PLA's T_g point. The values belonging to these endothermic peaks slightly decreased to 60.5, 61.6, and 61.2 °C after loading drugs in 8%, 12%, and 15% (w/v) NFs, respectively. T_m values of PLA in PNF8, PNF12, and PNF15 were observed at 155.1, 155.7, and 152.8 °C, respectively. After loading DO and CUR in NFs, there were no significant differences in T_m values of PLA, which were observed at 156.5, 156.7, and 154.2 °C for DNF8, DNF12, and DNF15, respectively. According to the literature, the glass transition temperature of PCL, which is around −60 °C, was not observed in the current working range.[45] In the DSC analysis, DNFs showed lower T_g values compared to PNFs, and this change may be derived from chemical or physical interactions between drugs and polymers.[46,47] Also, the working temperature ranges between T_g and T_m slightly increased by loading DO and CUR in NFs.[48] Additionally, the T_m values of CUR and DO were reported as 175 °C[49] and 227 °C,[18] respectively. But, the T_m values could not be detected in DSC graphs due to the low amount of drugs compared to polymers and homogeneous distribution of drugs in the formulation.[50] These results demonstrate that

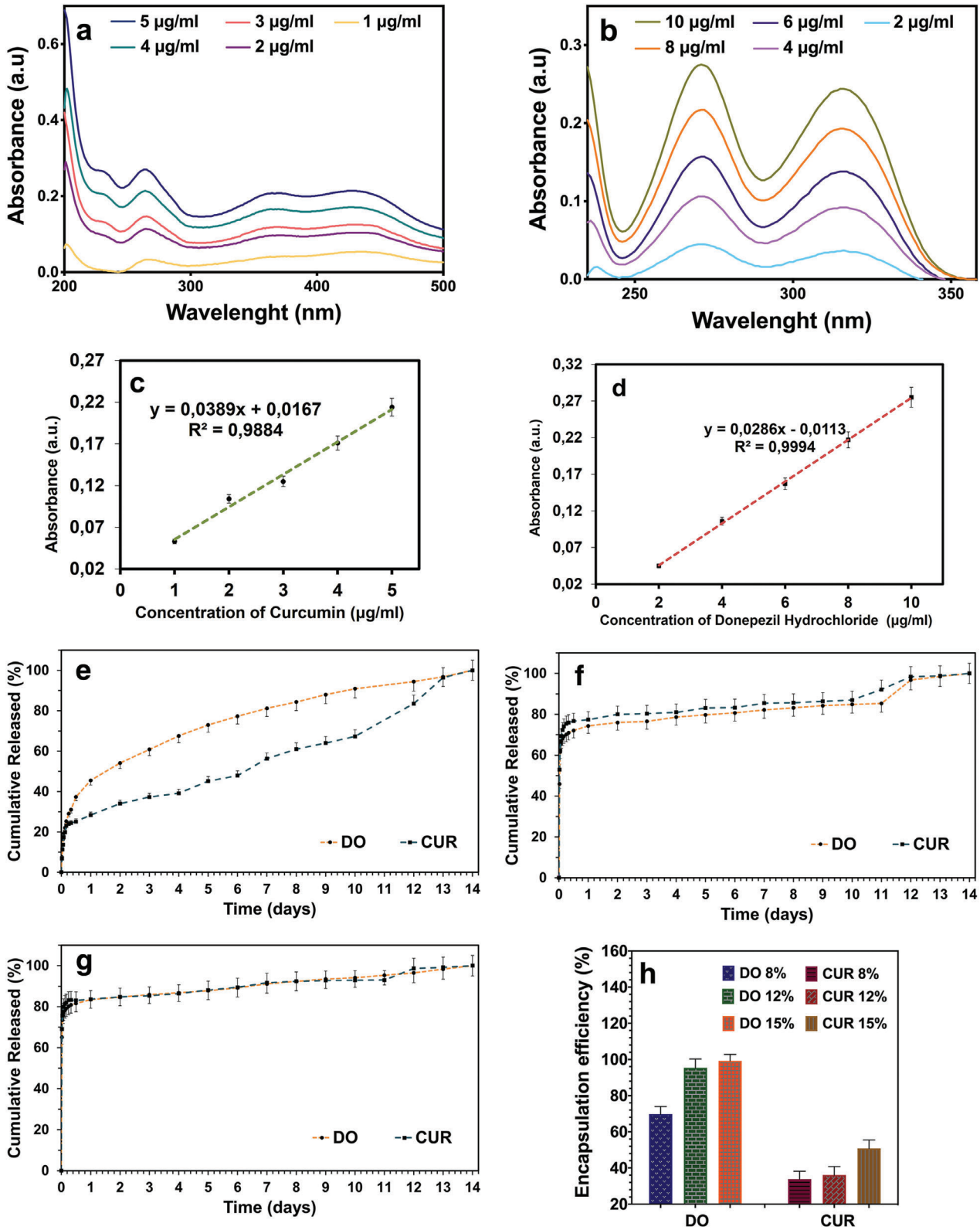

Figure 4. In vitro drug release profiles of nanofibers (NFs). a) Absorption spectra of curcumin (CUR) at different concentrations. b) Absorption spectra of donepezil (DO) at different concentrations. c) CUR calibration curves. d) DO calibration curves. e) DO and CUR release profiles from DO/CUR-loaded 8% polylactic acid (PLA)/polycaprolactone (PCL) NFs (DNF8). f) CUR and DO release profiles from DO/CUR-loaded 12% PLA/PCL NFs (DNF12). g) CUR and DO release profiles from DO/CUR-loaded 15% PLA/PCL NFs (DNF15) during 14 days. h) Encapsulation efficiency of DO/CUR-loaded PLA/PCL NFs (8%, 12%, and 15%). The experiments were repeated three times (relative error less than 5%).

Table 3. Results of mathematical drug release models for all nanofibers (NFs). CUR 8%: curcumin released from 8% polylactic acid/polycaprolactone (PLA/PCL) NFs. DO 8%: donepezil released from 8% PLA/PCL NFs. CUR 12%: curcumin released from 12% PLA/PCL NFs. DO 12%: donepezil released from 8% PLA/PCL NFs. CUR 15%: curcumin released from 15% PLA/PCL NFs. DO 15%: donepezil release from 15% PLA/PCL NFs.

	Zero order		First order		Hixson–Crowell	
Sample	R^2	K_0	R^2	K_1	R^2	K_{HC}
CUR 8%	0.9592	0.2354	0.7253	−0.0036	0.7932	0.0084
DO 8%	0.8813	0.2574	0.9220	−0.0044	0.9347	0.0098
CUR 12%	0.4077	0.1071	0.7524	−0.0036	0.7203	0.0065
DO 12%	0.4553	0.1116	0.7252	−0.0033	0.7007	0.0063
CUR 15%	0.2722	0.0868	0.7743	−0.0035	0.6825	0.0061
DO 15%	0.3123	0.0937	0.8457	−0.0033	0.7208	0.0061

all NFs can be safely applied into human body without the risk of melting.

3.7. Tensile Test of NFs

Tensile behaviors of NFs are influenced by the interaction between each polymer and the chemical structure of materials.[51] Strain at break and tensile strength of three samples of each PNF8, PNF12, PNF15, DNF8, DNF12, and DNF15 were examined, and the results are given in Figure 3c,d. It was found that the tensile strength of PNFs (8%, 12%, and 15%, w/v) were 295.5 ± 72.3, 246.5 ± 22.4, and 124.7 ± 42.6 kPa, respectively. In addition, when drugs were loaded in PNFs, the tensile strength of NFs increased to 611.4 ± 49.2, 535.0 ± 30.9, and 398.6 ± 17.6 kPa, respectively (Figure 3c). The strain at breaks of PNFs (8%, 12%, and 15%, w/v) were 39.2 ± 0.7%, 37.1 ± 2.0%, and 30.7 ± 6.5%, respectively. After loading of DO and CUR to PNFs, the strain at breaks of NFs were 15.2 ± 3.2%, 13.9 ± 0.7%, and 11.7 ± 0.5%, respectively (Figure 3d). Due to drugs (DO, CUR) having crystalline structures resulted in DNFs having higher tensile strength but lower structural flexibility than PNFs.[52] Furthermore, it was noticed that the tensile strength decreased by increasing the diameter of NFs.[53] Withal, DNFs were found suitable as a drug delivery system according to the tensile test.

3.8. In Vitro Drug Release Test

An in vitro drug release test was performed to study the release profiles of drugs from NFs. For this, DNF8, DNF12, and DNF15 were analyzed for 14 days. In the beginning, the linear standard calibration curves of DO and CUR solutions were constructed. After that, the EEs were measured as 69.8%, 95.3%, and 99.2% for DO and 33.89%, 36.1%, and 50.8% for CUR at DNF8, DNF12, and DNF15, respectively. It was obtained that the EE% was raised by increasing NF diameters. According to the results of Camerlo et al., these results were found similar.[54] PBS at 37 °C and pH 7.4 was used during the study to create an environment similar to the physiological conditions of living organisms.[54] About 28.4% of CUR and 45.5% of DO were released from DNF8 in the first 24 h. While 56.2% of CUR was released within 7 days, 54.1% of DO was released after 48 h from DNF8. A sustained release continued for 14 days in these NFs. For DNF12, they showed a burst release profile by releasing 62.4% of CUR and 61.5% of DO of their ingredients in 1 h. Also, sustained drug release was observed after 1 h for 14 days in these NFs. Moreover, DNF15 exhibited a higher burst release profile by releasing their 75.7% of CUR and 73.5% of DO off all ingredients in 1 h compared to DNF12. These NFs also showed a sustained release for 14 days. Thus, it was proven that increases in diameters of NFs boost the initial drug burst release ratio of NFs (**Figure 4**). These changes in drug release behaviors may come out of different swelling behavior and drug diffusion of NFs bearing various diameters.[55,56] Besides, the porosity of NFs affects the drug release profiles. A faster drug release is performed by thicker NFs due to their higher porosity. Our results were found to be in compatible with the literature.[57] As shown in previous studies, PLA fibers have porous structure,[58] and the porosity in NFs increases with the increase of PLA ratio in NF. Therefore, DNF15 displayed faster drug release with higher porosity compared to lower ratios.

Zero-order, first-order, and Hixson–Crowell release models were used to analyze the release kinetics of DO and CUR from all NF samples incubated in dynamic conditions of PBS at pH 7.4, 37 °C. The zero-order model is defined as drug release via a drug delivery system that releases its ingredient at a constant rate independent of its concentration, and the time is the only function for drug release. The first order is described as a drug release model in which the drug release is dependent on the remaining drug concentration. The Hixson–Crowell model is explained as a system in which the cube root of the released amount of the encapsulated drug is linearly related to the time, and in this system, the surface alters by time.[59]

The drug release constant (K) decreases with increasing polymer contents.[60] In the current study, similar trends were observed and K decreased with zero-order and Hixson–Crowell drug release kinetic models by increasing polymer concentration from 8% to 15%. There was no significant difference in K values between samples in the first-order kinetic model (**Table 3**). CUR with higher R^2 values was released from PLA/PCL NFs at 8% by the zero-order model, at 12% and 15% by the first-order model (Table 3). On the other hand, it was found that Hixson–Crowell and first-order models demonstrated a preferable consonance with higher R^2 values of DO for 8%; and 12% and 15% PLA/PCL NFs, respectively. Drug release kinetic results for the 8% ratio are given in **Figure 5**, and for 12% and 15% ratios are

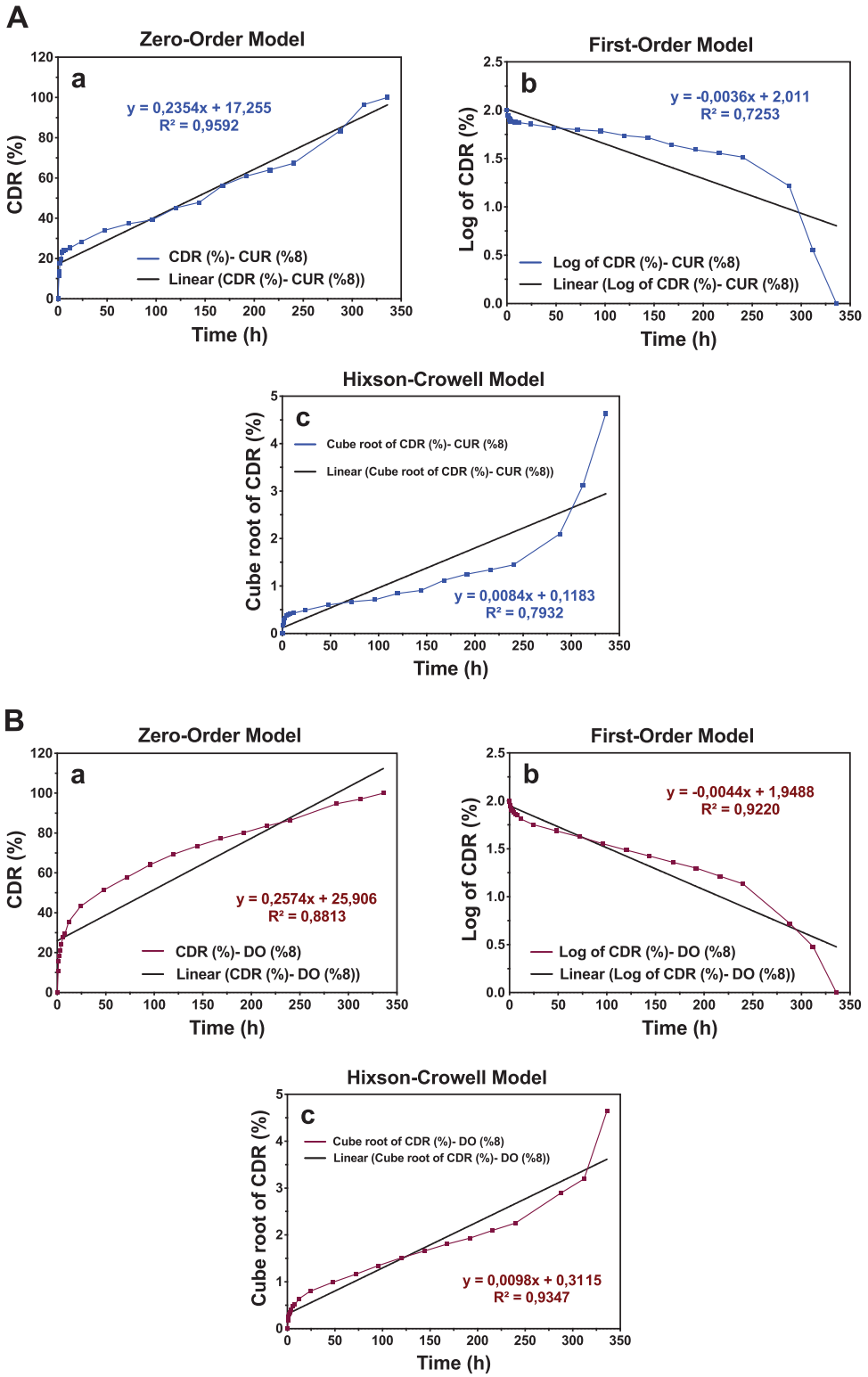

Figure 5. The release kinetic models of A) curcumin (CUR) and B) donepezil (DO) release profiles from DO/CUR-loaded 8% polylactic acid (PLA)/polycaprolactone (PCL) nanofibers for 14 days: a) zero-order, b) first-order, and c) Hixson–Crowell models.

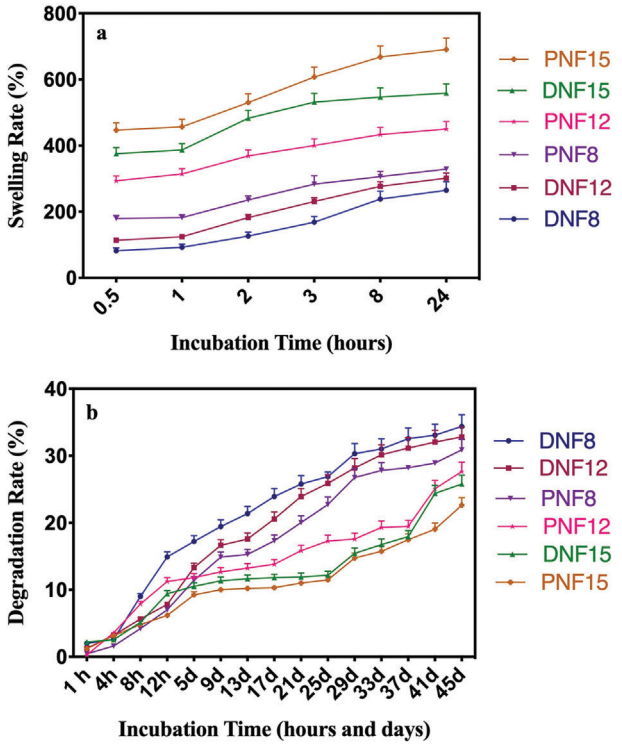

Figure 6. a) Swelling rate and b) degradation rate of all nanofibers (NFs) in phosphate-buffered saline (PBS). DNF8: donepezil/curcumin (DO/CUR)-loaded 8% polylactic acid (PLA)/polycaprolactone (PCL) NFs, DNF12: DO/CUR-loaded 12% PLA/PCL NFs, DNF15: DO/CUR-loaded 15% PLA/PCL NFs, PNF8: pure 8% PLA/PCL NFs, PNF12: pure 12% PLA/PCL NFs, and PNF15: pure 15% PLA/PCL NFs.

given in Figures S3 and S4 (Supporting Information), respectively.

3.9. Swelling Test

The swelling rate is one of the factors affecting drug release kinetics. The swelling ratio of polymers and their water uptake capacity are directly proportional to each other. PLA and PCL have low water uptake capacities because of their hydrophobic nature. The swelling ratios of PNFs and DNFs are shown in **Figure 6**a. It was observed that PNF15 showed more swelling properties compared to the other NFs. Furthermore, it was noted that their weights were approximately seven times (691.0%) heavier compared to their initial weights. The swelling percentages of PNF8 and PNF12 ratios by the end of 24 h were measured as 329.0% and 450.5%, respectively. The swelling rates of DNF15, DNF12, and DNF8 were 559.1%, 301.6%, and 264.8%, respectively. It was analyzed that the diameter raised as the polymer concentration increased, so the swelling behaviors improved due to the increase in the diameter.[61]

3.10. Degradation Test

All samples were immersed at different intervals in PBS (pH 7.4) to determine the degradation of the NFs as a critical parameter in the drug release behavior of the NFs.[62] Some studies last up to 7 months in the literature because PCL and PLA polymers have a long degradation time.[63,64] In this study, a 45 day degradation test was performed. Degradation rates of all NFs are shown in Figure 6b. In a study by Haroosh et al., the degradation rate of PLA/PCL polymer composite was found to be 6.30%, while the ratios of polymer composite in this study were nearly between 10% and 15% on the 14th day of the degradation test. The reason for *t* slow degradation has been considered to semicrystalline nature of PCL.[65] On the 45th day, PNF8, PNF12, and PNF15 degraded at the rates of 30.9%, 27.7%, and 22.6%, respectively. Degradation percentages of DNF8, DNF12, and DNF15 on the 45th day of the degradation test were 34.1%, 32.8%, and 25.8%, respectively; It was proved that the degradation rate decreased with the increase of NF diameter.[66] The degradation rate of DNFs is higher than that of PNFs since the surface contact of the PBS and the NF is increased by the channels created by the drugs released from the NFs.[65] Furthermore, the loading of drugs, which has hydrophilic properties, in fibers increased their degradation in all three ratios compared to PNFs.

3.11. Evaluation of Cell Viability

In this study, the effects of polymer concentrations on cell viability were compared to the drugs loaded in NFs at the same concentration. Healthy mouse fibroblast cells (L929) were used for the cytotoxicity test of NFs, and no cytotoxic effect was found (**Figure 7**a). It has been proven by SEM that a suitable environment was provided for the proliferation and growth of fibroblast cell clusters (Figure 7b–g). The cell viability decreased on PNFs by the increase of polymer concentration.[67] On the other hand, it was found that DNF12 had the highest cell viability effect. Consequently, all NF samples could be used in further animal tests or biomedical applications due to their good cytocompatibility effect. In addition to all this, DNF12 could be chosen as the most suitable vehicle due to cell viability results.

4. Conclusion

In our study, DO and CUR were combined in NFs for creating an innovative dual-acting drug delivery system for the treatment of AD. The diameters of NFs decreased by the decrease of polymer concentration and in the case of loading drugs. The swelling ratio and encapsulation efficiency increased; degradation ratio and tensile strength decreased with the increase of fiber diameter. A higher initial drug burst release ratio was observed in DNFs by the increase of fiber diameter due to their higher porosity. The drugs were released from PLA/PCL NFs at all polymer concentrations according to the first-order model. Furthermore, the tensile strength increased, and the flexibility decreased by loading drugs in NFs due to the drugs' crystalline structures. The T_m value of NFs increased but the T_g value decreased by loading drugs in NFs. Besides, there is no cytotoxicity on mouse fibroblast cell clusters at all polymer concentrations but only DNF12 increased the cell viability proliferation compared to other NFs. Consequently, fiber diameter has affected all characteristic features of NFs, and DNFs could be used as a new and promising drug delivery system for the treatment of AD.

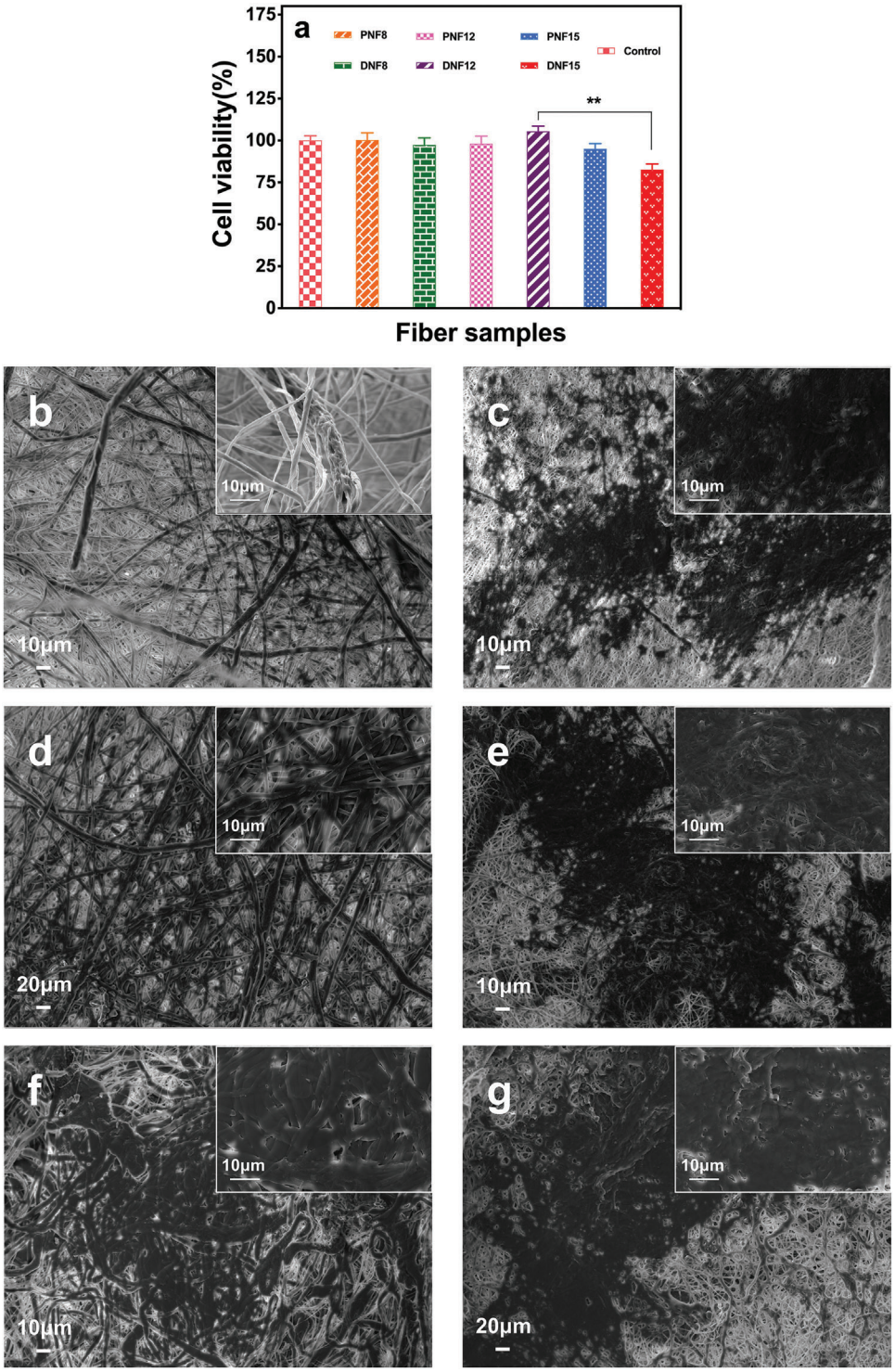

Figure 7. a) L929 (mouse fibroblast) cell viability of all samples. The data are presented as mean ± standard error of the mean. $^{**}p < 0.01$ versus the control group. SEM images of proliferated cells on b) pure 8% polylactic acid (PLA)/polycaprolactone (PCL) nanofibers (NFs) (PNF8), c) donepezil (DO)/curcumin (CUR)-loaded 8% PLA/PCL NFs (DNF8), d) pure 12% PLA/PCL NFs (PNF12), e) DO/CUR-loaded 12% PLA/PCL NFs (DNF12), f) pure 15% PLA/PCL NFs (PNF15), and g) DO/CUR-loaded 15% PLA/PCL NFs (DNF15).

Supporting Information

Supporting Information is available from the Wiley Online Library or from the author.

Acknowledgements

This project was supported by a TUBITAK 2209-A Research Projects Program (Grant Nos. 2209-A, 2020/2, 1919B012002602, Scientific and Technological Research Council of Turkey-TUBITAK).

Conflict of Interest

The authors declare no conflict of interest.

Author Contributions

S.A. and I.K. contributed equally to this work. The manuscript was written through the contributions of all authors. All authors have approved the final version of the manuscript.

Data Availability Statement

The data that support the findings of this study are available from the corresponding author upon reasonable request.

Keywords

Alzheimer's disease, curcumin, donepezil hydrochloride, electrospinning, nanofibers

Received: November 14, 2021
Revised: February 7, 2022
Published online: March 6, 2022

[1] C. A. Lane, J. Hardy, J. M. Schott, *Eur. J. Neurol.* **2018**, *25*, 59.
[2] Y.-G. Chen, *Chin. Med. J.* **2018**, *131*, 1618.
[3] H. Hampel, M. M. Mesulam, A. C. Cuello, M. R. Farlow, E. Giacobini, G. T. Grossberg, A. S. Khachaturian, A. Vergallo, E. Cavedo, P. J. Snyder, Z. S. Khachaturian, *Brain* **2018**, *141*, 1917.
[4] Alzheimer's Association, *Alzheimers Dement.* **2020**, *16*, 391.
[5] M. Cam, T. Taskin, *Clin. Exp. Health Sci.* **2020**, *10*, 93.
[6] H. Niu, I. Álvarez-Álvarez, F. Guillén-Grima, I. Aguinaga-Ontoso, *J. Neurol.* **2017**, *32*, 523.
[7] B. Seltzer, *Expert Opin. Drug Metab. Toxicol.* **2005**, *1*, 527.
[8] S. D. Voulgaropoulou, T. A. M. J. Van Amelsvoort, J. Prickaerts, C. Vingerhoets, *Brain Res.* **2019**, *1725*, 146476.
[9] M. Chen, Z. Y. Du, X. Zheng, D. L. Li, R. P. Zhou, K. Zhang, *Neural Regen. Res.* **2018**, *13*, 742.
[10] H. Alenezi, M. E. Cam, M. Edirisinghe, *Appl. Phys. Rev.* **2019**, *6*, 041401.
[11] N. Turuvekere Vittala Murthy, V. Agrahari, H. Chauhan, *Eur. J. Pharm. Biopharm.* **2021**, *161*, 66.
[12] R. Xu, Z. Zhang, M. S. Toftdal, A. C. Møller, F. Dagnaes-Hansen, M. Dong, J. S. Thomsen, A. Brüel, M. Chen, *J. Controlled Release* **2019**, *301*, 129.
[13] A. Luraghi, F. Peri, L. Moroni, *J. Controlled Release* **2021**, *334*, 463.
[14] S. Sabra, D. M. Ragab, M. M. Agwa, S. Rohani, *Eur. J. Pharm. Sci.* **2020**, *144*, 105224.
[15] A. Khalf, S. V. Madihally, *Eur. J. Pharm. Biopharm.* **2017**, *112*, 1.
[16] M. Herrero-Herrero, J. A. Gómez-Tejedor, A. Vallés-Lluch, *Eur. Polym. J.* **2018**, *99*, 445.
[17] P. S. C. Sacchetin, R. F. Setti, P. D. T. V. E. Rosa, Â. M. Moraes, *Mater. Sci. Eng., C* **2016**, *58*, 870.
[18] A. Gencturk, E. Kahraman, S. Güngör, G. Özhan, Y. Özsoy, A. S. Sarac, *Artif. Cells, Nanomed., Biotechnol.* **2017**, *45*, 655.
[19] K. Anjireddy, S. Karpagam, *Int. J. Biol. Macromol.* **2017**, *105*, 131.
[20] G. Perumal, S. Pappuru, D. Chakraborty, A. Maya Nandkumar, D. K. Chand, M. Doble, *Mater. Sci. Eng., C* **2017**, *76*, 1196.
[21] F. Sahne, M. Mohammadi, G. Najafpour, A. Moghadamnia, *J. Biotechnol.* **2016**, *13*, 173.
[22] M. E. Cam, S. Yildiz, H. Alenezi, S. Cesur, G. S. Ozcan, G. Erdemir, U. Edirisinghe, D. Akakin, D. S. Kuruca, L. Kabasakal, O. Gunduz, M. Edirisinghe, *J. R. Soc., Interface* **2020**, *17*, 20190712.
[23] S. Md, M. Ali, S. Baboota, J. K. Sahni, A. Bhatnagar, J. Ali, *Drug Dev. Ind. Pharm.* **2014**, *40*, 278.
[24] M. Bhatia, M. Saini, *Prog. Biomater.* **2018**, *7*, 239.
[25] C. Aguzzi, P. Cerezo, I. Salcedo-Bellido, R. Snchez, C. Viseras, *Mater. Technol.* **2010**, *25*, 205.
[26] E. Ilhan, S. Cesur, E. Guler, F. Topal, D. Albayrak, M. M. Guncu, M. E. Cam, T. Taskin, H. T. Sasmazel, B. Aksu, F. N. Oktar, O. Gunduz, *Int. J. Biol. Macromol.* **2020**, *161*, 1040.
[27] P. Heseltine, J. Ahmed, M. Edirisinghe, *Macromol. Mater. Eng.* **2018**, *303*, 1800218.
[28] F. S. Alfares, E. Guler, H. Alenezi, M. E. Cam, M. Edirisinghe, *Macromol. Mater. Eng.* **2021**, *306*, 2100471.
[29] A. Haider, S. Haider, I.-K. Kang, *Arabian J. Chem.* **2018**, *11*, 1165.
[30] W. K. Son, J. H. Youk, T. S. Lee, W. H. Park, *Polymer* **2004**, *45*, 2959.
[31] M. E. Cam, B. Ertas, H. Alenezi, A. N. Hazar-Yavuz, S. Cesur, G. S. Ozcan, C. Ekentok, E. Guler, C. Katsakouli, Z. Demirbas, D. Akakin, M. S. Eroglu, L. Kabasakal, O. Gunduz, M. Edirisinghe, *Mater. Sci. Eng., C* **2021**, *119*, 111586.
[32] C. Drosou, M. Krokida, C. G. Biliaderis, *Food Hydrocolloids* **2018**, *77*, 726.
[33] C. Mit-Uppatham, M. Nithitanakul, P. Supaphol, *Macromol. Chem. Phys.* **2004**, *205*, 2327.
[34] J. K. Park, Y. B. Choy, J. M. Oh, J. Y. Kim, S. J. Hwang, J. H. Choy, *Int. J. Pharm.* **2008**, *359*, 198.
[35] X. Chen, L.-Q. Zou, J. Niu, W. Liu, S.-F. Peng, C.-M. Liu, *Molecules* **2015**, *20*, 14293.
[36] W. Guo, P. Quan, L. Fang, D. Cun, M. Yang, *Asian J. Pharm. Sci.* **2015**, *10*, 405.
[37] S. Dhanasekaran, P. Rameshthangam, S. Venkatesan, S. K. Singh, S. R. Vijayan, *J. Polym. Environ.* **2018**, *26*, 4095.
[38] K.-T. Chen, K. Nguyen, C. Ieritano, F. Gao, Y. Seimbille, *Molecules* **2018**, *24*, 23.
[39] H. Jeong, J. Rho, J.-Y. Shin, D. Y. Lee, T. Hwang, K. J. Kim, *Biomed. Eng. Lett.* **2018**, *8*, 267.
[40] M. E. Cam, A. N. Hazar-Yavuz, S. Cesur, O. Ozkan, H. Alenezi, H. Turkoglu Sasmazel, M. Sayip Eroglu, F. Brako, J. Ahmed, L. Kabasakal, G. Ren, O. Gunduz, M. Edirisinghe, *Int. J. Pharm.* **2020**, *588*, 119782.
[41] H. Sun, A. Xiao, B. Yu, G. Bhat, F. Zhu, *Polymer* **2017**, *41*, 181.
[42] J. M. Deitzel, J. Kleinmeyer, D. Harris, N. C. Beck Tan, *Polymer* **2001**, *42*, 261.
[43] E. Torres, A. Gaona, N. García-Bosch, M. Muñoz, V. Fombuena, R. Moriana, A. Vallés-Lluch, *Polymers* **2021**, *13*, 2475.
[44] M. Cristea, D. Ionita, M. M. Iftime, *Materials* **2020**, *13*, 5302.
[45] V. R. Sinha, K. Bansal, R. Kaushik, R. Kumria, A. Trehan, *Int. J. Pharm.* **2004**, *278*, 1.
[46] E. M. Abdelrazek, I. S. Elashmawi, S. Labeeb, *Phys. B* **2010**, *405*, 2021.

[47] A. Abdelghany, M. A. Morsi, A. Abdelrazek, M. T. Ahmed, *Silicon* **2018**, *10*, 519.
[48] K. K. Gupta, N. Pal, P. K. Mishra, P. Srivastava, S. Mohanty, P. Maiti, *J. Biomed. Mater. Res., Part A* **2014**, *102*, 2600.
[49] Z. Sayyar, H. Jafarizadeh, *Int. J. Food Eng.* **2019**, *15*, 1.
[50] F. Bahadori, Z. Eskandari, N. Ebrahimi, M. S. Bostan, M. S. Eroğlu, E. T. Oner, *Eur. J. Pharm. Sci.* **2019**, *138*, 105037.
[51] A. Ricci, K. J. Olejar, G. P. Parpinello, P. A. Kilmartin, A. Versari, *Appl. Spectrosc. Rev.* **2015**, *50*, 407.
[52] A. Y. Abdolmaleki, H. Zilouei, S. N. Khorasani, K. Zargoosh, *Water Sci. Technol.* **2018**, *77*, 1324.
[53] M. E. Cam, S. Cesur, T. Taskin, G. Erdemir, D. S. Kuruca, Y. M. Sahin, L. Kabasakal, O. Gunduz, *Eur. Polym. J.* **2019**, *120*, 109239.
[54] A. Camerlo, C. Vebert-Nardin, R. M. Rossi, A.-M. Popa, *Eur. Polym. J.* **2013**, *49*, 3806.
[55] A. Doustgani, *J. Ind. Text.* **2017**, *47*, 71.
[56] V. Pillay, C. Dott, Y. E. Choonara, C. Tyagi, L. Tomar, P. Kumar, L. C. du Toit, V. M. K. Ndesendo, *J. Nanomater.* **2013**, *2013*, 789289.
[57] S. Thakkar, M. Misra, *Eur. J. Pharm. Sci.* **2017**, *107*, 148.
[58] L. Liu, Z. Lin, J. Niu, D. Tian, J. He, *Adsorpt. Sci. Technol.* **2019**, *37*, 438.
[59] L. Pourtalebi Jahromi, M. Ghazali, H. Ashrafi, A. Azadi, *Heliyon* **2020**, *6*, e03451.
[60] I. Jiménez-Martínez, T. Quirino-Barreda, L. Villafuerte-Robles, *Int. J. Pharm.* **2008**, *362*, 37.
[61] H.-Y. Lin, Y.-J. Kuo, S.-H. Chang, T.-S. Ni, *Biomed. Mater.* **2013**, *8*, 025009.
[62] B. Pant, M. Park, S.-J. Park, *Pharmaceutics* **2019**, *11*, 305.
[63] A. C. Vieira, J. C. Vieira, R. M. Guedes, A. T. Marques, *Mater. Sci. Forum* **2010**, *636*, 825.
[64] M. Milosevic, D. B. Stojanovic, V. Simic, M. Grkovic, M. Bjelovic, P. S. Uskokovic, M. Kojic, *Sci. Rep.* **2020**, *10*, 11126.
[65] H. J. Haroosh, Y. Dong, K.-T. Lau, *J. Mater. Sci.* **2014**, *49*, 6270.
[66] Y. Dong, S. Liao, M. Ngiam, C. K. Chan, S. Ramakrishna, *Tissue Eng., Part B* **2009**, *15*, 333.
[67] E. Martín-López, M. Nieto-Díaz, M. Nieto-Sampedro, *J. Appl. Biomater. Funct. Mater.* **2013**, *11*, e151.